15 August 2002

ELSEVIER

Optics Communications 209 (2002) 397–401

OPTICS COMMUNICATIONS

www.elsevier.com/locate/optcom

# Efficient compact watt-level deep-ultraviolet laser generated from a multi-kHz Q-switched diode-pumped solid-state laser system

L.B. Chang[a,*], S.C. Wang[a], A.H. Kung[a,b]

[a] *Institute of Electro-Optical Engineering, National Chiao Tung University, Hsinchu 30050, Taiwan, ROC*
[b] *Institute of Atomic and Molecular Sciences, Academia Sinica, Taipei 106, Taiwan, ROC*

Received 5 March 2002; received in revised form 2 June 2002; accepted 10 June 2002

**Abstract**

Stable high-power operation in the deep ultraviolet is achieved from a multi-kHz diode-pumped multi-longitudinal-mode Q-switched Nd:YAG laser by fourth harmonic generation in an external resonant cavity and by fifth harmonic generation using sum-frequency mixing of the fourth harmonic and the residual fundamental in a β-BBO crystal. Over 2.1 W of 266 nm radiation and 540 mW of 213 nm radiation were generated from a fundamental power of 7 W of 1064 nm light at 5 kHz. The overall conversion efficiency from IR to deep ultraviolet at 213 nm is larger than 7.5%. 

*PACS:* 42.65.Ky; 42.60.Da; 42.79.Nv

*Keywords:* Laser; Nonlinear optics; Frequency conversion; Harmonic generation

All-solid-state deep-ultraviolet (DUV) coherent sources with watt level and high repetition rate are needed for applications such as lithography alignment, disk mastering, grating fabrication, mask fabrication, etc. Up until now most of the solid-state high power DUV coherent sources are achieved by cascaded single-pass harmonic generation using either a giant pulse system [1–4], or a tightly focused, relatively complicated arrangement for compact diode-pumped systems [5–8]. Serious thermal distortion associated with tightly focused beam arrangement in high average power situations has limited their acceptance in application to date [5–7]. One approach to overcome these limitations is to use resonant cavity enhancement in harmonic generation [9]. The external enhancement cavity permits the use of a larger beam size than in the single-pass arrangement to achieve a similar conversion efficiency for the same average input and output power. This means that the size of the fourth harmonic beam generated in the case of cavity enhancement is several times larger than that generated in the single-pass case. In addition,

* Corresponding author. Tel.: +886-2-2366-8270; fax: +886-2-2362-0200.
*E-mail address:* lbzhang@pchome.com.tw (L.B. Chang).

0030-4018/02/$ - see front matter 
PII: S0030-4018(02)01669-3

the resonance condition increases the UV pulse duration. As a result, the peak power density of the UV pulse for the resonant case is significantly lower than that for the single-pass case. Since the primary source of thermal distortion and BBO crystal damage is UV absorption at 266 nm, the use of external cavity enhancement can therefore alleviate these problems and extend the life of the optics used in the generation process. In previous communications, we have reported on fourth harmonic UV generation by incorporating two doubling stages inside a single external ring cavity [10–12]. This arrangement allows the cavity to resonate at the second harmonic frequency, which simplifies the optical requirement on the coupling of the fundamental beam into the cavity.

Here, we report the application of this new technique to generate over 2 W at 266 nm and more than 0.5 W at 213 nm from a laser diode-pumped Nd:YAG laser, requiring only relatively simple and straightforward configuration that allows long term operation. The overall conversion efficiency from IR to DUV at 213 nm is larger than 7.5%.

Fig. 1 illustrates the optical configuration used in this experiment. The pump laser was a multi-kHz diode-pumped multi-longitudinal-mode Q-switched Nd:YAG laser at 1064 nm (Lightwave Electronics model 611–1064). A half-wave plate was used to adjust the orientation of the polarization of the 1064 nm radiation for optimizing the harmonic generation processes. The harmonic generation cavity was formed by mirrors M1, M2 and M3 which were highly reflecting ($R > 99.5\%$) at 532 nm. The fundamental beam was coupled into the ring cavity through the mirror M1. M1 and M2 were flat and highly transmitting at 1064 nm ($T \sim 98\%$) and 266 nm ($T \sim 90\%$), respectively. M3 was mounted on a PZT crystal driven holder and had a 2.0 m radius of curvature. A necessary condition for external cavity resonance enhancement is to match the phase of the fundamental light with that of the second harmonic light at the entrance face of the second harmonic generation (SHG) crystal. This condition is satisfied by maintaining the cavity length to better than about $\pm 1/20$ of a wavelength ($\pm 0.025$ μm) on resonance with an electronic feed-forward servo-control system that drives the PZT crystal [12]. In addition, for multi-longitudinal mode pump lasers, the mode spacing of the external cavity must be set to match that of the pump laser cavity to realize the enhancement [10]. The tolerance on the length of the optical cavity due to this requirement is a fraction of the coherence length of the laser, which is a few mm for the Nd:YAG laser.

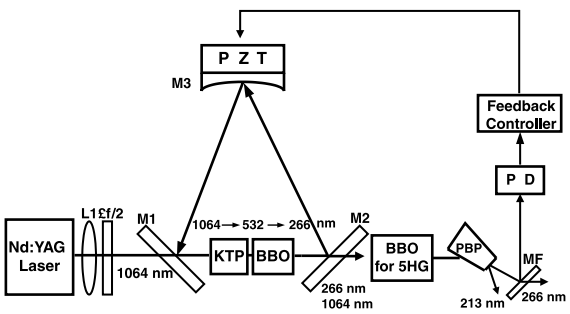


Fig. 1. Experimental arrangement for the FHG in a resonant cavity and 5HG. L1 – lens, FI – Faraday isolator, $\lambda/2$ – half-wave plate, M1–M3 – mirrors, PBP – Pellin-Broca prism, MF – $MgF_2$ plate, PD – photodiode, PZT – piezoelectric transducer.

The SHG crystal was a $3 \times 3 \times 5$ mm$^3$ type-II KTP whose end faces were dual antireflection coated for 1064 and 532 nm. It is oriented so that the generated light is vertically polarized. The crystal for fourth harmonic generation (FHG) was a $4 \times 4 \times 6.8$ mm$^3$ type-I BBO crystal that was dual antireflection coated for 532 and 266 nm. For an input linearly polarized at 45°, the 266 nm generated was horizontally polarized. The fundamental and 266 nm beams exited the cavity from M2. A BBO crystal cut for type-I phase-matched summing of these beams to 213 nm was placed at ~5 cm from this mirror. This BBO crystal was $4 \times 4 \times 7$ mm$^3$ in size and had a protective coating against moisture damage on both end faces. A Pellin Broca prism was used to separate the different beams (1064, 266 and 213 nm) at the final output location. A small portion of the 266 nm was sampled as the input signal for the servo controller. The output powers were measured by a calibrated thermopile with a one-second time constant. The thermopile output was recorded and plotted using Origin 5.0 data analysis software. The entire system fits within a 1 m$^2$ area on a vibration-isolated table.

The pulse width of 1064 nm light was 23.3 ns with a single pulse energy of 1.4 mJ, measured just in front of the KTP crystal. The pulse repetition rate was 5 kHz. The IR beam was focused to a Gaussian waist radius of 0.44 mm. The SHG and FHG crystals were located close to the waist position. The resulting peak input power density was 19.8 MW/cm$^2$.

The FHG process was first studied. Both single-pass and resonance-enhanced performances were recorded. Under optimized alignment, 164 mW single-pass and 1.89 W of enhanced output were obtained immediately in front of the last BBO crystal. After making corrections for surface reflections and mirror transmission losses, the resonantly enhanced internal generation at 266 nm was about 2.1 W, corresponding to an internal conversion efficiency from 1064 nm of 30% at a relatively safe input power density of 19.8 MW/cm$^2$. In this optical configuration, the FHG beam coming out from M2 is collinear with the residual fundamental beam. As a result, the fifth harmonic at 213 nm could be generated by mixing the 266 nm beam with the horizontally polarized component of the residual fundamental beam immediately outside the resonant cavity. No additional optics would be required. However, proper attention must be paid to the spatial and temporal overlaps of these input beams. It is well known that BBO has a large beam walk-off angle of 4.84° [13]. The fundamental beam and the fourth harmonic beam were being separated spatially as they propagated through the FHG crystal due to this birefringent walk-off. Beam separation occurred also inside the mirror M2 due to an oblique angle of incidence (45°). With proper orientation of the FHG crystal's axis, the walk-off produced by FHG can compensate the walk-off caused by M2 [14], thus helping to improve the spatial overlap of the two beams (see Fig. 2). If the crystal were flipped by 180°, the separation of the two beams would become additive and the overlap would get worse.

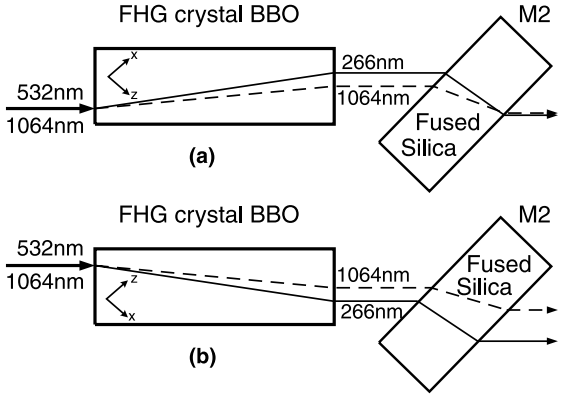


Fig. 2. Walk-offs produced by a 6.8-mm birefringent crystal and the output coupler M2. Both 1064 and 266 nm lights are horizontally polarized, and 532 nm light is vertically polarized: (a) crystal oriented to reduce beam separation; (b) crystal oriented 180° from (a), showing increased separation.

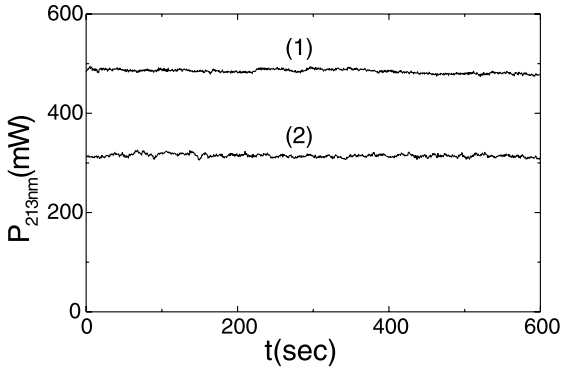


Fig. 3. The comparison of output power at 213 nm for two different orientation of the FHG BBO. Curve (1) with FHG BBO oriented to enhance 266 and 1064 nm beam overlap. Curve (2) with the BBO crystal axis flipped 180°.

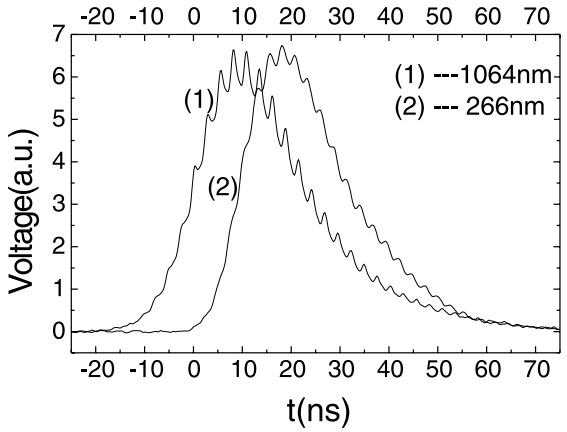


Fig. 4. The 266 nm pulse duration was about 22 ns with its peak delayed by ~8 ns from the peak of a 1064 nm pulse which duration was about 25.2 ns.

Table 1
A comparison of the output power of 213 nm and the powers of the 4HG and the fundamental light that are injected to the last BBO crystal

| $f = 5$ kHz | Residual $P_{1064\ nm}$ (measured) | $P_{266\ nm}$ (measured) | $P_{213\ nm}$ (measured) |
|---|---|---|---|
| Single-pass | 5.9 W | 154 mW | 65 mW |
| Resonant-enhanced, before adjusting the half-wave plate | 3.5 W | 1.72 W | 345 mW |
| Resonant-enhanced, after adjusting the half-wave plate | 4 W | 1.6 W | 484 mW |

For a 6.8 mm long crystal and a 0.25 in. thick $SiO_2$ substrate for M2, the proper compensation amounted to a difference of 54% in 213 nm output power as shown in Fig. 3, which shows the fifth harmonic generation (5HG) power as a function of time for both cases. The gradual decrease of power with time was due to a slow degradation of the protective coating at the input face of the 5HG crystal inflicted by the high power at 266 nm. A solution to this damage problem is not to use the protective coating and leave the crystal uncoated. However, in doing so, it is necessary to keep the crystal at an elevated temperature to keep moisture away from the polished faces of the hygroscopic crystal.

The 266 nm pulse duration was 22 ns with its peak delayed by ~8 ns from the 1064 nm peak shown in Fig. 4. Correction to the temporal difference between the two pulses is more complicated. It would involve separating the two pulses, inserting an 8 ns delay for one, and then recombining the two. In an effort to maintain a simple and compact arrangement, we opted not to make this correction. Since the pulse duration is over 20 ns, the negative connotation of this effect is calculated to be less than 10%. There is another physical phenomenon, pertinent to the resonant enhancement arrangement, which has an important consequence to the 5HG. With the FHG conversion optimized, the portion of the fundamental suitable for frequency conversion was substantially depleted (>50%). Furthermore, only the horizontally polarized component (50%) of the residual 1064 nm power could be used because the polarization at 1064 nm must be oriented at 45° to the horizontal axis to accommodate type-II phase-matching in the SHG stage. We took advantage of this fact to alleviate the problem of a partially depleted pump in the 5HG process. We rotated the half-wave plate away from its optimal position for FHG. This resulted in slightly lower FHG power output, but the adjustment reserved a portion of the 1064 nm power, making it available for the 5HG process. Experimentally, this rotation was only a few degrees. Table 1 shows the measured UV outputs for single-pass and the resonant enhancement cases. With the FHG crystal properly oriented, and the half-wave plate adjusted to the optimized angle, we obtained a 5HG output of 484 mW from a fundamental power of 7 W. After making corrections for Fresnel losses, the internal generation was over 540 mW, and this corresponds to a conversion efficiency of 7.7%. It is clear that after adjustment of the half-wave plate, the 213 nm power increased by 40% over the power before the adjustment, and was 7.4 times as much as the power of the single-pass case.

## Acknowledgements

We thank the National Science Council and the Ministry of Education of Taiwan for their partial support.

## References

[1] T. Kojima, S. Konno, S. Fujikawa, K. Yasui, K. Yoshizawa, Opt. Lett. 25 (2000) 58.
[2] S.V. Murav'ev, A.A. Babin, F.I. Fel'dshtein, A.M. Yurkin, V.A. Kamensky, A.Yu. Malyshev, M.S. Kitai, N.M. Bityurin, Quantum Electron. 28 (1998) 520.
[3] R. Wu, M.J. Myers, J.D. Myers, S.J. Hamlin, in: C. Payne, C. Pollock (Eds.), OSA TOPS on Advanced Solid-State Lasers, vol. 1, 1996, p. 349.

[4] M. Oka, H. Masuda, H. Kikuchi, S. Kubota, in: Lasers and Electro-Optics Society Annual Meeting, LEOS 96, IEEE, vol. 2, 1996, p. 358.
[5] U. Stamm, W. Zschocke, T. Schroder, N. Deutsch, D. Basting, Technical Digest of CLEO'97, 1997, Paper CFE7, p. 481.
[6] S. Kubota, H. Masuda, H. Kikuchi, M. Oka, J. Alexander, Technical Digest of CLEO'97, 1997, Paper CFM3, p. 511.
[7] J.C. Garcia, A.K. Newman, J.M. Liu, M.C. Lee, J. Opt. A: Pure Appl. Opt. 2 (2000) L41.
[8] J. Sakuma, K. Deki, A. Finch, Y. Ohsako, T. Yokota, Appl. Opt. 39 (2000) 5505.
[9] A. Ashkin, G.D. Boyd, J.M. Dziedzic, IEEE J. Quantum Electron. QE-2 (1966) 109.
[10] A.H. Kung, J.I. Lee, P.J. Chen, Appl. Phys. Lett. 72 (1998) 1542.
[11] J. Knittel, A.H. Kung, Opt. Lett. 22 (1997) 366.
[12] J. Knittel, A.H. Kung, IEEE J. Quantum Electron. 33 (1997) 2021.
[13] I. Shoji, H. Nakamura, K. Ohdaira, T. Kondo, R. Ito, T. Okamoto, K. Tatsuki, S. Kubota, J. Opt. Soc. Am. B 16 (1999) 1968.
[14] L.K. Samanta, T. Yanagawa, Y. Yamamoto, Opt. Commun. 76 (1990) 250.